Overexpression of Periostin and Distinct Mesothelin Forms Predict Malignant Progression in a Rat Cholangiocarcinoma Model

Miguel Á. Manzanares, Deanna J.W. Campbell, Gabrielle T. Maldonado, and Alphonse E. Sirica

Periostin and mesothelin have each been suggested to be predictors of poor survival for patients with intrahepatic cholangiocarcinoma, although the clinical prognostic value of both of these biomarkers remains uncertain. The aim of the current study was to investigate these biomarkers for their potential to act as tumor progression factors when assessed in orthotopic tumor and three-dimensional culture models of rat cholangiocarcinoma progression. Using our orthotopic model, we demonstrated a strong positive correlation between tumor and serum periostin and mesothelin and increasing liver tumor mass and associated peritoneal metastases that also reflected differences in cholangiocarcinoma cell aggressiveness and malignant grade. Periostin immunostaining was most prominent in the desmoplastic stroma of larger sized more aggressive liver tumors and peritoneal metastases. In comparison, mesothelin was more highly expressed in the cholangiocarcinoma cells; the slower growing more highly differentiated liver tumors exhibited a luminal cancer cell surface immunostaining for this biomarker, and the rapidly growing less differentiated liver and metastatic tumor masses largely showed cytoplasmic mesothelin immunoreactivity. Two molecular weight forms of mesothelin were identified, one at ~40 kDa and the other, a more heavily glycosylated form, at ~50 kDa. Increased expression of the 40-kDa mesothelin over that of the 50 kDa form predicted increased malignant progression in both the orthotopic liver tumors and in cholangiocarcinoma cells of different malignant potential in three-dimensional culture. Moreover, coculturing of cancer-associated myofibroblasts with cholangiocarcinoma cells promoted overexpression of the 40-kDa mesothelin, which correlated with enhanced malignant progression *in vitro*. *Conclusion*: Periostin and mesothelin are useful predictors of tumor progression in our rat desmoplastic cholangiocarcinoma models. This supports their relevance to human intrahepatic cholangiocarcinoma. (*Hepatology Communications* 2018;2:155-172)

Introduction

Intrahepatic cholangiocarcinoma (ICC) is a primary epithelial cancer of the hepatobiliary tract that exhibits variable histopathologic features and biomarkers of cholangiocyte differentiation.[1] Most ICCs are mass-forming tumors, with 90%-95% classified as high-to-moderate-to low grade adenocarcinomas. They are commonly characterized by a prominent desmoplastic stroma populated by α-smooth muscle actin-positive cancer-associated fibroblasts (α-SMA + CAFs).[2] These cancers frequently metastasize, with intrahepatic, lymphatic, peritoneal, and lung metastases being common recurrence sites in patients with ICC and resectable cancer.[3]

Currently, there are no curative systemic medical therapies for ICC,[4] and even in those cases where curative-intent hepatic tumor resection is an option, recurrence rates have been reported to range between 40% and 80%.[5] Moreover, considering the insidious onset of ICC and the fact that a majority of patients with ICC do not meet the criteria for curative-intent

Abbreviations: 3-D, three-dimensional; α-SMA + CAFs, α-smooth muscle actin-positive cancer-associated fibroblasts; BDEsp cells, spontaneously transformed BDE1 cholangiocytes; ELISA, enzyme- linked immunosorbent assay; FBS, fetal bovine serum; HCC, hepatocellular carcinoma; ICC, intrahepatic cholangiocarcinoma; Msln, mesothelin; PCNA, proliferating cell nuclear antigen; PNGaseF, peptide N-glycosidase F; Postn, periostin.

Received July 13, 2017; accepted November 14, 2017.
Additional Supporting Information may be found at onlinelibrary.wiley.com/doi/10.1002/hep4.1131/full.
Supported by National Institutes of Health Grant R01 CA083650 to A.E.S.

resection because of advanced disease at the time of diagnosis, there is a critical need to identify and validate biomarker signatures associated with increased ICC aggressiveness. The ultimate aim is to devise more effective strategies for the clinical management of advanced or recurrent ICC. In this context, the matricellular glycoprotein periostin (Postn) and the glycosylphosphatidylinositol-anchored cell membrane glycoprotein mesothelin (Msln) have each been independently suggested as having potential as prognostic factors for human ICC.[6,7] Each may also provide opportunities for the development of novel targeted therapies for ICC.[8,9]

Postn has been shown in both human and rat ICCs to be produced solely by α-SMA + CAFs in the ICC stroma.[6,8] Its potential as an independent prognostic risk factor for poor survival for patients with ICC was first suggested by Utispan et al.,[6] who demonstrated that surgically resected ICC patients with tumors strongly immunostained for CAF-Postn had significantly shorter postoperative survival times than those expressing low levels of Postn. Benign liver diseases (e.g., liver cirrhosis, focal nodular hyperplasia) were further reported to show no-to-slight Postn immunoreactivity, and Postn expression was not detected in the cancer cells of conventional hepatocellular carcinoma (HCC).[6,10] Patients with cholangiocarcinoma were also reported to exhibit a significantly higher median Postn level in their serum than those with normal liver, liver cirrhosis, HCC, or other malignancies.[10] High serum and tumor tissue samples with high Postn expression detected by immunohistochemistry have been significantly associated with reduced survival in patients with ICC,[11] which suggests that elevated serum Postn may be used to divide such patients into low and high Postn groups.

Msln was reported to be localized by immunohistochemistry to the cholangiocarcinoma cells of human ICC.[9] Furthermore, 32%-37% of analyzed cases of human ICCs have been determined to overexpress Msln,[7,9,12] which was either not detected or only occasionally and weakly seen in HCC[9,12] and not observed in normal adult human liver tissue samples.[9] Patients with ICC with resected tumors containing ≥50% Msln-positive cholangiocarcinoma cells exhibited a significantly shorter postoperative survival than those exhibiting Msln negativity or focal positivity,[7] suggesting Msln overexpression to be a prognostic factor in patients undergoing hepatectomy for ICC.

Although the findings described above implicate increased Postn and Msln expression as being associated with poor survival outcomes in ICC, their suggested value as possible independent biomarkers of ICC progression remains uncertain due in part to potential limitations in single-center study designs as well as to inconsistencies in reported findings from other clinical research groups. Notably, in their systematic review and meta-analysis to investigate the prognostic value of immunohistochemically based biomarkers that have been assessed in patients with resected ICC, Ruys et al.[13] graded the study of Utispan et al.[6] on Postn as having a high risk of bias based on defined criteria to evaluate publication bias for biomarkers. Also, in contrast to the findings of Nomura et al.,[7] Higashi

View this article online at wileyonlinelibrary.com.
DOI 10.1002/hep4.1131

Potential conflict of interest: Nothing to report.

ARTICLE INFORMATION:

From the Division of Cellular and Molecular Pathogenesis, Department of Pathology, Virginia Commonwealth University School of Medicine, Richmond, VA.

ADDRESS CORRESPONDENCE AND REPRINT REQUESTS TO:

Alphonse E. Sirica, Ph.D., M.S.
Division of Cellular and Molecular Pathogenesis,
Department of Pathology
Virginia Commonwealth University School of Medicine
P.O. Box 980297
Richmond, VA 23298-0297
E-mail: alphonse.sirica@vcuhealth.org
Tel: +1-804-828-9549

et al.[14] observed no significant difference in survival on resected ICC patients with Msln-positive tumors compared with those that were Msln negative. In addition, in a single-center clinical study involving nine human cases of biliary cancers, median serum Msln was not elevated over that determined for healthy donors.[15] Moreover, only one[9] of the human studies published to date used western blotting to assess and validate individual levels of Msln protein being expressed in individual ICC specimens; instead these other studies relied solely on immunostaining to score tumors with high versus low levels of expression.

To our knowledge, no reported studies have investigated the expression patterns and modulation of Postn and/or Msln in relation to tumor progression in either experimental animal or cell culture models of cholangiocarcinoma. In this context, we have now used a "patient-like" orthotopic rat model of cholangiocarcinoma progression developed in our laboratory[16] as well as our more recently described three-dimensional (3-D) culture model of rat desmoplastic cholangiocarcinoma[17] to further evaluate under controlled experimental conditions the potential predictive value of Postn and Msln overexpression as indicators of increasing cholangiocarcinoma growth and progression. In addition, we have identified two Msln forms distinguished by differences in their molecular weight (~50 kDa and ~40 kDa) and glycosylation properties, which allowed us to differentiate the lower malignant grade cholangiocarcinoma tumors and cancer cells from those of increased malignant grade.

Materials and Methods

CELL LINES/STRAINS AND CULTURE CONDITIONS

The highly tumorigenic rat BDEneu cholangiocyte cell line and the rat TDEcc cholangiocarcinoma cell strain used in this study were previously established in our laboratory and have been extensively characterized.[16-19] Briefly, the BDEneu cell line was established by stably transfecting a well-differentiated, high-passaged, but nontumorigenic rat cholangiocyte cell line (BDE1), initially developed in the laboratory of Dr. Douglas Hixson,[20] with the mutationally activated transforming rat *erbB2/neu* oncogene (Glu664-*neu*).[18] The rat TDE_{CC} cholangiocarcinoma cell strain was derived from a well-differentiated desmoplastic cholangiocarcinoma formed in syngeneic, young adult male, Fischer 344 rat liver following bile duct inoculation of spontaneously transformed BDE1 cholangiocytes (BDEsp cells), as described.[17] A novel clonal strain of α-SMA + CAFs, designated TDF_{SM}, was also established from the same orthotopic rat desmoplastic cholangiocarcinoma type as the TDE_{CC} cell strain and was comparatively characterized in terms of its distinct biological, karyotypic, phenotypic, molecular, and functional properties.[17] Similarly, we established an epithelial cell line (BDEneu-Met) from a BDEneu peritoneal metastasis according to the same method used by us to establish the TDE_{CC} cholangiocarcinoma cell strain. The human bile duct cancer cell lines analyzed in this study included the commercially available HuCCT1 ICC cell line purchased from the Japan Health Science Foundation and the human bile duct carcinoma cell line EGI-1 obtained from the German Collection of Microorganisms and Cell Cultures (Braunschweig, Germany).

Each of the cell lines (rat and human) were either cultured on rat-tail collagen type I-coated plastic culture dishes or within 3-D collagen type I hydrogel matrix, as described.[17] Organotypic 3-D TDE_{CC} + TDF_{SM} cocultures were established as described.[17] For each cell culture experiment, the cells were maintained in our standard medium comprised of Dulbecco's modified Eagle's medium supplemented with penicillin (100 U/mL), streptomycin (100 μg/mL), insulin (0.1 μmol/L), transferrin (5 μg/mL), and 10% fetal bovine serum (FBS).

ORTHOTOPIC RAT CHOLANGIOCARCINOMA MODEL

All animal experimentation for this study was performed in accordance with the corresponding author's currently active protocol AD10000625 approved by Virginia Commonwealth University's Institutional and Animal Care and Use Committee. The orthotopic rat model of mass-forming ICC progression used in this study, based on bile duct inoculation of tumorigenic rat cholangiocyte cell lines/strains (e.g., BDEneu, TDE_{CC}, BDEsp) of different malignant cell growth rates and metastatic potential into the left hepatic lobes of syngeneic young adult male Fischer 344 rats, is well described.[16-19] Briefly, rats having a mean body weight of 256.7 ± 19.7 g were subjected under ketamine/xylazine anesthesia to bile duct inoculation of 5×10^6 BDEneu cells (mean cell viability, 94.6% ± 2.9%) in 0.1% Hank's balanced salt solution into liver,

according to our detailed protocol.[16] Resulting tumor-bearing rats were then euthanized over a 10- to 22-day period after initial cell inoculation with an intraperitoneal lethal injection of Euthasol from Virginia Commonwealth University's Division of Animal Resources. Cardiac puncture under deep terminal anesthesia was used to obtain blood samples for serum preparation. Corresponding samples of total gross liver tumor tissue and total pooled amounts of gross peritoneal metastases as well as pair-matched right liver lobe tissue without tumor were collected by careful dissection from fully euthanized rats. The individual rat liver tumors and associated pooled peritoneal metastases were grouped by wet weight for subsequent analyses. Control liver and serum samples were obtained from normal rats. In addition, formalin-fixed, paraffin-embedded, liver tumor tissue samples prepared from cholangiocarcinoma that had formed in rat liver at ~50 days after bile duct inoculation into liver of either 10×10^6 viable rat TDE_{CC} cholangiocarcinoma cells[17] or at ~40-76 days in rats orthotopically transplanted with 4×10^6 rat BDEsp cells[16] were processed for Postn and Msln immunohistochemistry.

IMMUNOHISTOCHEMISTRY

Immunohistochemistry of Postn and Msln was carried out as described[17] on histologic sections prepared from formalin-fixed paraffin embedded tissue samples of rat ICC tumors, peritoneal metastasis, and pair-matched liver tissue specimens without tumor. Likewise, Msln immunostaining was performed on histologic sections from 3-D collagen-I hydrogel cultures of TDE_{CC}, BDEneu, and BDEneu-Met cells as well as on histologic sections prepared from TDE_{CC}, TDF_{SM}, and TDE_{CC} + TDF_{SM} gel cultures. The following primary antibodies were used: anti-rat C-expressed in renal carcinoma/mesothelin (306) rabbit immunoglobulin G-affinity purified (code no. 28001; Clontech Laboratories, Inc., Mountain View, CA) and anti-periostin rabbit polyclonal antibody (ab92460; Abcam, Inc., Cambridge, MA). Proliferating cell nuclear antigen (PCNA) immunostaining of tumor samples was carried out as described.[17]

WESTERN BLOT ANALYSIS

Western blot analysis was performed on total protein lysates prepared from either rat tumor or control liver tissues or from cell protein lysates prepared from 2-D or 3-D cell cultures, as described.[17] The primary Postn and Msln antibodies used for western blotting were the same as those described above for immunohistochemistry. Protein bands were normalized to either actin (cat no. A2066; Sigma-Aldrich, Inc.) or to vinculin (cat no. ab129002; Abcam) and quantified as described.[17]

Postn AND Msln ENZYME-LINKED IMMUNOSORBENT ASSAYS

Serum samples separated from whole blood obtained from individual rats were aliquoted and immediately frozen at −80 °C. Enzyme-linked immunosorbent assays (ELISAs) for Postn and N-ERC/Msln were performed on 1X, thawed, aliquoted samples using the Rat periostin/osteoblast specific factor 2 (POSTN) ELISA Kit (cat. no. MBS706561; My BioSource, Inc., San Diego, CA) and the Rat N-ERC/Mesothelin Assay kit (code no. 27765; IBL Co., Ltd., Spring Lake Park, MN), according to the manufacturers' instructions. This latter assay kit detects the N-terminal fragment of full-length Msln.

ENZYMATIC CLEAVAGE OF Msln N-GLYCAN SITES

Protein extraction samples from cultured BDEneu and TDE_{CC} cells were comparatively treated with recombinant peptide N-glycosidase F (PNGaseF) (cat no. P0708S; New England BioLabs, Inc., Ipswich, MA) to hydrolyze N-glycan chains from Msln. Protein samples (40 μg) from the respective cell types were incubated overnight in a final volume of 20 μL with 1 μg of enzyme at 37 °C, according to the manufacturer's recommendations. Controls included enzyme without cell protein and sample protein without enzyme. Following enzyme incubation, protein samples were heated at 80 °C for 10 minutes in the presence of dithiothreitol, and the total reaction volume was loaded and analyzed by western blotting for differences in Msln protein banding patterns.

STATISTICAL ANALYSES

For the bar graph representations, the Student two-tailed *t* test was used to determine *P* values. In the case of linear graphic representations, Pearson correlation analysis was used to calculate *r* and *P* values. In both cases, $P \leq 0.05$ was considered significant. Graphic data are presented as means ± SD. Additional details are given in the figure legends.

Results

CORRELATION BETWEEN ORTHOTOPIC CHOLANGIOCARCINOMA MASS IN LIVER AND PERITONEAL METASTATIC TUMOR MASS

Consistent with our earlier findings,[16] bile duct inoculation of BDEneu cells into the left lateral liver lobes of syngeneic Fischer 344 male rats yielded small gross intrahepatic tumors at around 10 days after cell inoculation, followed over the next 10-12 days by rapid exponential growth of liver tumor, together with concomitant increases in gross peritoneal metastases (Fig. 1A). We could demonstrate a strong positive correlation between mean liver tumor wet weight and pooled peritoneal metastases wet weight ($r = 0.9994$; $P = 1.8 \times 10^{-5}$), indicative of increasing malignant progression as a function of larger liver tumor size (Fig. 1B). Distinct areas of necrosis were typically not significant in any of the analyzed tumor specimens, which were grossly composed of hard white masses of high-malignant grade desmoplastic cholangiocarcinoma when compared with moderately differentiated TDE_{CC} and well-differentiated BDEsp cholangiocarcinomas (Supporting Fig. S1). Every effort was taken to only use tissue samples without gross or microscopic evidence of necrosis in our immunohistochemical and western blot analyses. Representative examples of PCNA labeling of high-grade versus low-grade rat liver cholangiocarcinoma tumor types analyzed are shown in Supporting Fig. S2.

IMMUNOHISTOCHEMICAL PATTERNS OF Postn AND Msln EXPRESSION REFLECT DIFFERENCES IN CHOLANGIOCARCINOMA TUMOR DIFFERENTIATION

Postn immunoreactivity was confined solely to tumor stroma and not detected in the cholangiocarcinoma cells in sections from the different sized BDEneu liver tumors and from individual peritoneal metastases (Fig. 2A). Stromal Postn immunostaining was more prominent in sections prepared from the larger sized tumors and from associated peritoneal metastases compared to those prepared from the small liver tumors (Fig. 2A). In comparison, the cholangiocarcinoma cells of the small liver tumors were observed to be strongly immunoreactive for Msln, which was either not detected or only weakly detected in the stroma of these tumors. However, stromal Msln immunostaining became more prominent with increasing BDEneu liver tumor size and in associated peritoneal metastases but still noticeably weaker than that exhibited by the cholangiocarcinoma cells in these analyzed sections (Fig. 2A). Random histologic sections of pair-matched right liver lobes without cholangiocarcinoma from BDEneu tumor-bearing rats as well as liver from normal untreated animals were each found to be immunohistochemically negative for both Postn and Msln.

We also comparatively analyzed samples of slow growing well-differentiated BDEsp tumors, intermediate growing well-to-moderately differentiated TDE_{CC} tumors, and rapidly growing less differentiated BDEneu tumors for differences in their Postn and Msln immunostaining patterns. Postn immunoreactivity was most extensive in the stroma of the BDEneu tumors, less extensive in the TDE_{CC} tumors, and least extensive in the BDEsp tumors (Fig. 2B). On the other hand, the cholangiocarcinoma cells of the well-differentiated BDEsp tumors were strongly immunoreactive for Msln, which showed a distinct apical/luminal cell surface staining pattern; essentially no Msln was detected in the stroma of these tumors. Nests of less differentiated cholangiocarcinoma cells within BDEneu liver tumor, while strongly immunoreactive for cytoplasmic Msln, did not show apical/luminal cell surface immunostaining for this biomarker (Fig. 2B). TDE_{CC} liver tumors presented an intermediate Msln immunostaining profile, being detected at the apical/luminal cell borders of some of the cholangiocarcinoma ductal structures formed within these tumors but with either no or only weak Msln immunostaining in their stroma.

TUMOR AND SERUM Postn AND Msln AS PREDICTORS OF PROGRESSIVE BDEneu CHOLANGIOCARCINOMA GROWTH

Consistent with the immunohistochemical data shown in Fig. 2, we determined through quantitative western blotting that the mean relative Postn protein band intensities ± SD obtained from measurements made on individual BDEneu liver tumors and on corresponding pooled samples of peritoneal metastases

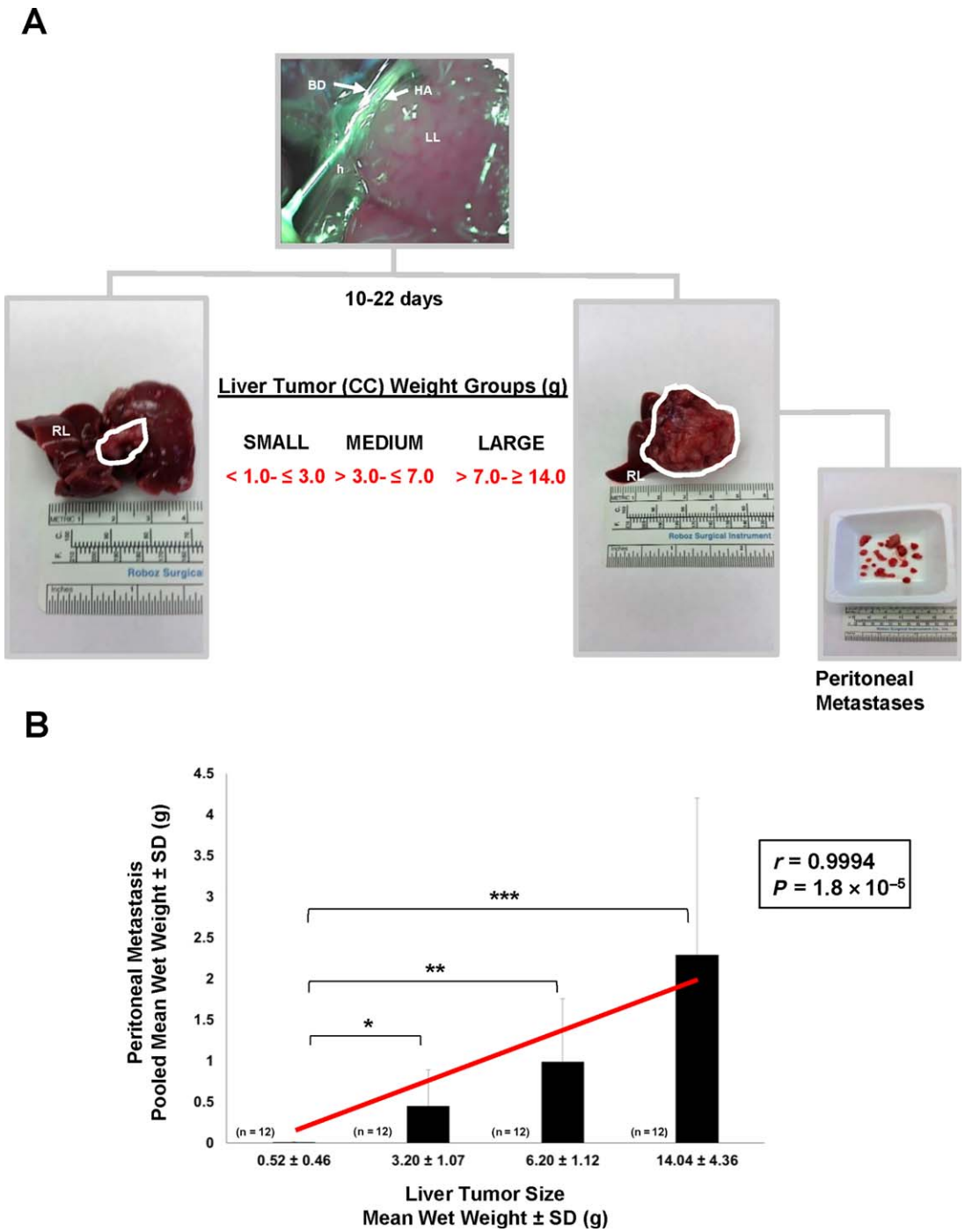

FIG. 1. Relationship between liver tumor size and peritoneal metastasis in the rat BDEneu cholangiocarcinoma model. (A) Bile duct inoculation of 5×10^6 rat BDEneu malignant neoplastic cholangiocytes at >90% viability directed through the left hepatic bile duct into the left liver lobe of young adult male syngeneic Fischer 344 rats resulted over a 10- to 22-day period in the formation of distinct mass-forming liver tumors ranging in size from small to large, with gross peritoneal metastases of various sizes being associated with the larger sized liver tumors. The smaller size liver tumors localized to the left hepatic lobe, whereas the largest sized tumors typically replaced much if not all of the normal left and median liver lobe tissue. The corresponding right liver lobe was typically free of gross tumor in this rat cholangiocarcinoma model. The left hepatic artery and hepatic hilus are labeled to help denote the positioning of the inserted inoculating needle. (B) Bar graph and corresponding linear regression curve, with Pearson's correlation coefficient (r) demonstrating a strong positive correlation between increasing mean liver tumor wet weight and increasing pooled mean gross peritoneal metastases wet weight in the BDEneu rat cholangiocarcinoma model. Wet weight measurements were made on entire amounts of liver tumor tissue and associated peritoneal metastases individually dissected from a total of 48 tumor-bearing rats; n, number of animals analyzed per liver tumor weight group; each bar value, mean ± SD. *$P \leq 2 \times 10^{-3}$, **$P \leq 2 \times 10^{-4}$, ***$P \leq 4 \times 10^{-4}$. Abbreviations: BD, bile duct; CC, cholangiocarcinoma; h, hepatic hilus; HA, left hepatic artery; LL, left liver lobe; RL, right liver lobe. Ruler Scale in mm, cm and inches.

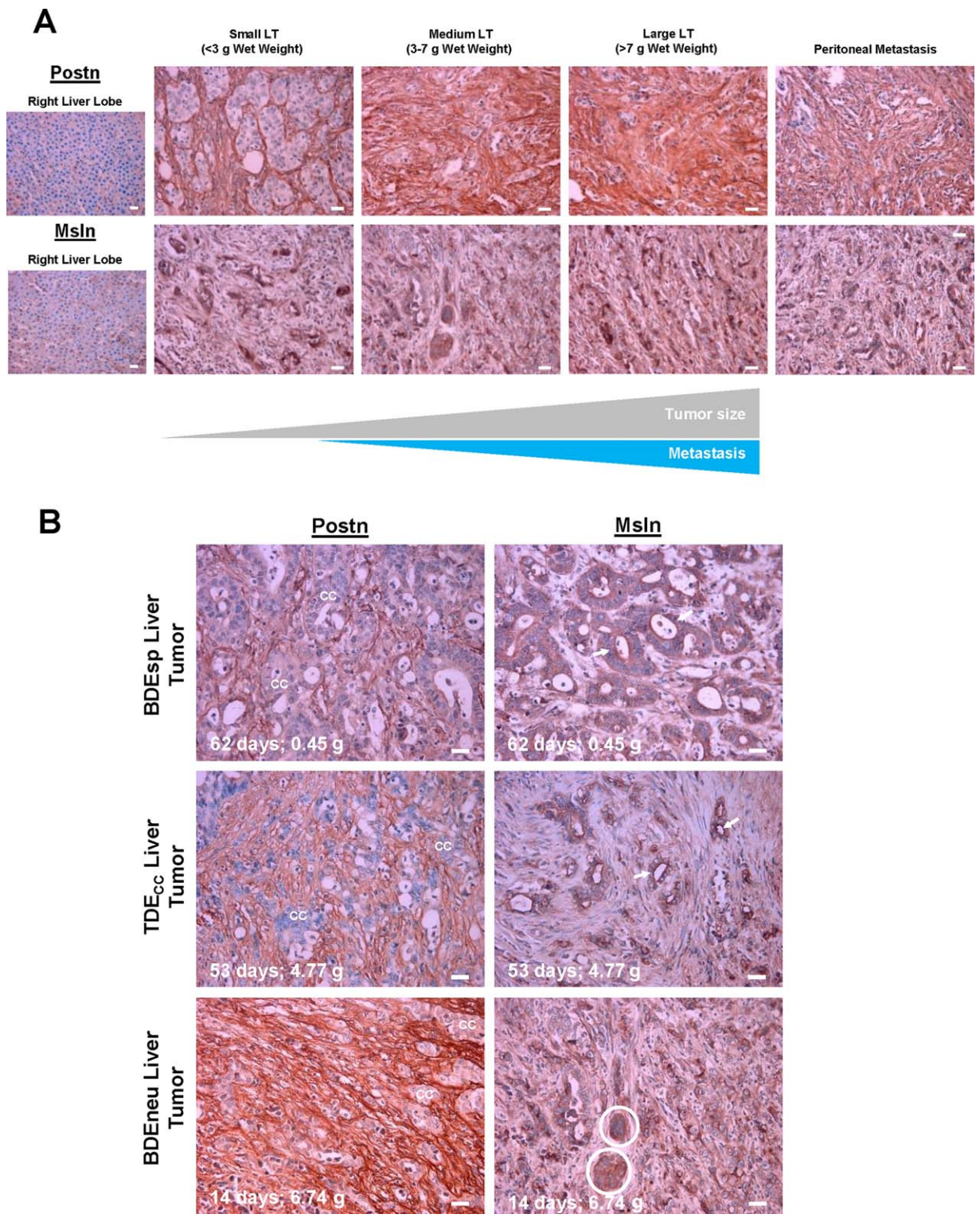

FIG. 2. Immunohistochemical patterns of expression of Postn and Msln in rat cholangiocarcinoma relative to increasing liver tumor size and grade and in associated peritoneal metastases. (A) Comparative patterns of Postn and Msln immunoreactivity in tissue sections of rat BDEneu liver tumors of increasing size versus those of associated peritoneal metastasis and corresponding right liver lobe without cholangiocarcinoma. (B) Differences in Postn and Msln immunostaining profiles characterizing slow growing well-differentiated BDEsp liver tumor, intermediate growing moderately differentiated TDE_{CC} liver tumor, and rapidly growing less differentiated BDEneu liver tumor. Days tumors harvested after initial bile duct inoculation of respective cholangiocarcinoma cell types and corresponding wet weights in grams are shown in each photomicrograph. cc and circled areas indicate cholangiocarcinoma; arrows point to luminal cell surface Msln immunoreactivity. Primary antibody dilutions: 1:200 for Postn and 1:400 for Msln. Controls without primary antibody were negative for Postn and Msln immunostaining (data not shown). Photomicrographs in A and B are representative of observations made on formalin-fixed paraffin-embedded tissue sections prepared from individual tissue samples from three to four tumor-bearing rats per tumor size group. Magnification bar = 20 μm. Abbreviations: cc, cholangiocarcinoma; LT, liver tumor.

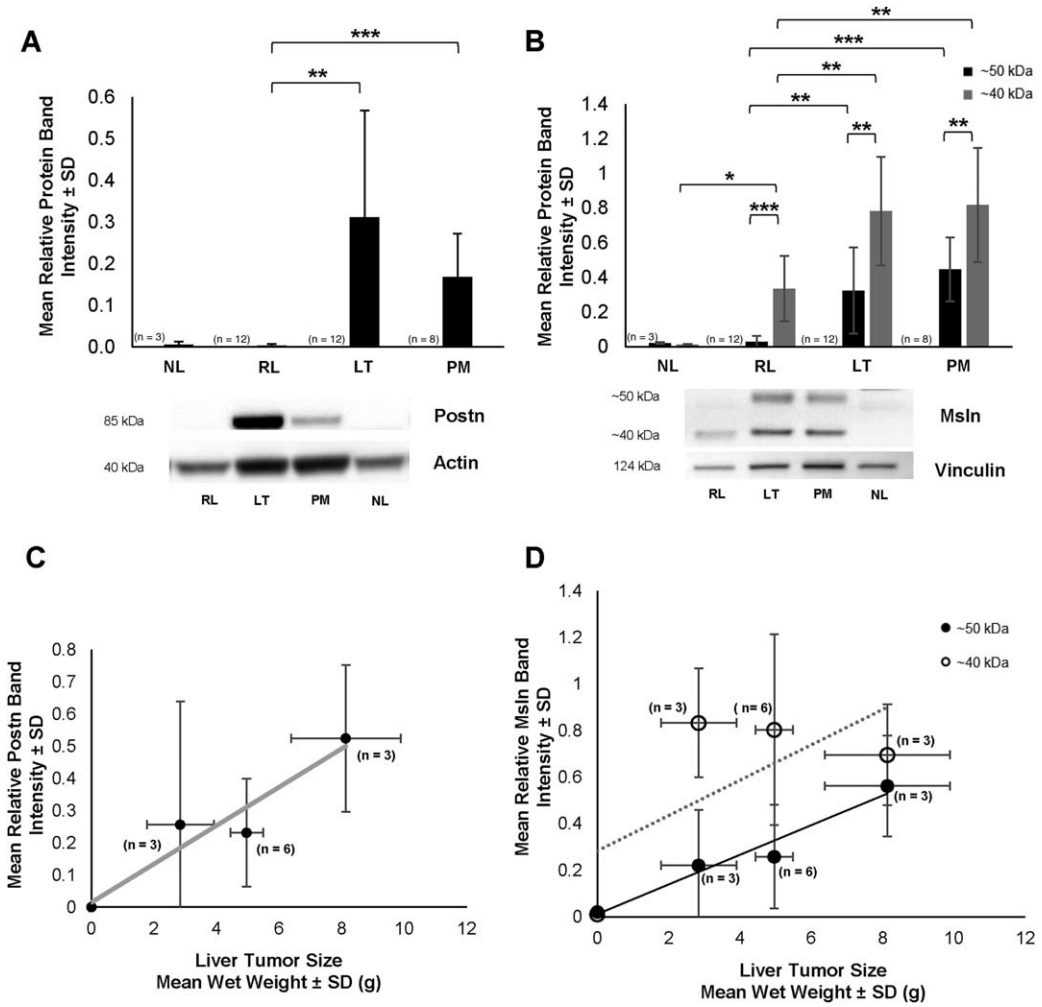

FIG. 3. Quantitative western blot analysis of Postn and Msln expression in the rat BDEneu cholangiocarcinoma model. (A) Bar graph demonstrating Postn overexpression in BDEneu liver tumor tissue and associated peritoneal metastases but not in corresponding right liver lobe tissue without cholangiocarcinoma or in liver tissue samples from normal untreated rats. (B) Differential overexpression of 50-kDa and 40-kDa forms of Msln in LT and PM, relative to RL and NL. $^{*}P \leq 1 \times 10^{-2}$, $^{**}P \leq 3 \times 10^{-4}$, $^{***}P \leq 3 \times 10^{-5}$. (C) Linear regression curve relating increases in BDEneu liver tumor size to increasing tumor Postn expression. Correlation coefficient $r = 0.954$; $P = 0.046$. (D) Linear regression curves reflecting a strong positive correlation between increasing BDEneu liver tumor size and increasing levels of 50-kDa Msln measured in the tumor tissue samples ($r = 0.977$; $P = 0.023$) versus a lack of correlation with levels of the 40-kDa Msln form ($r = 0.67$, $P = 0.328$). Postn and Msln band intensities were respectively normalized to actin or vinculin. Values in A-D represent mean ± SD; n, number of animals from which corresponding tissue specimens were individually obtained for western blot analyses. Abbreviations: LT, liver tumor; NL, normal liver; PM, peritoneal metastases; RL, right liver.

were each significantly increased over protein band intensities determined for tissue samples of pair-matched right liver lobe without evidence of gross tumor and for normal adult rat liver, neither of which exhibited detectable Postn protein bands (Fig. 3A). Two distinct Msln bands with molecular weights of ~50 and ~40 kDa were detected in both the BDEneu liver tumors and metastases (Fig. 3B), with the lower band (40 kDa) being expressed at a significantly higher mean relative protein band intensity level than that of the upper band (50 kDa). Although neither Msln bands were detected in the analyzed tissue samples from normal adult rat liver, we did detect a weak 40-kDa Msln band expressed in the pair-matched right liver lobe samples without evidence of cholangiocarcinoma obtained from these tumor-bearing rats.

As a further assessment, we analyzed our western blot data for Postn and Msln in relation to increasing

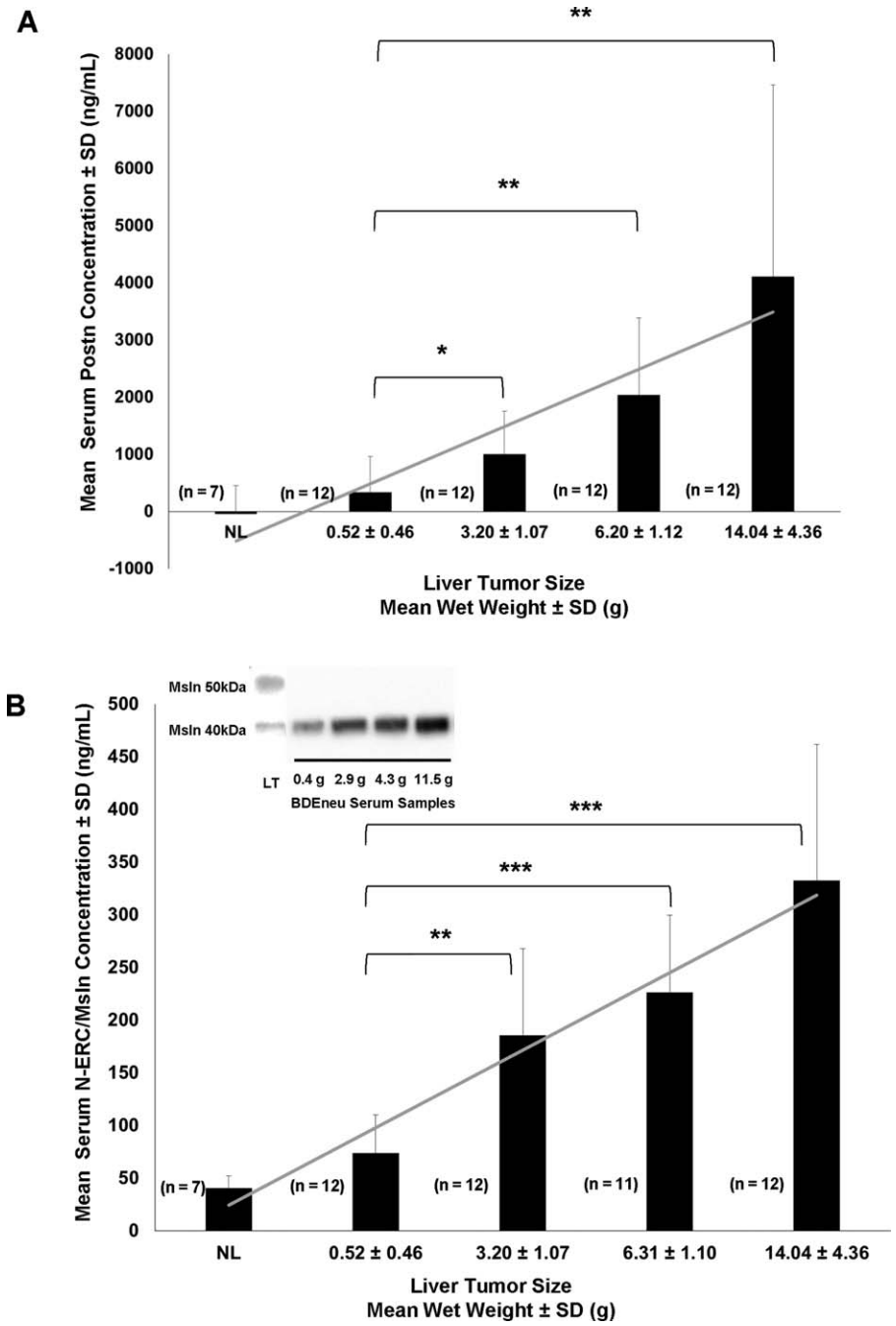

FIG. 4. Serum Postn and Msln levels significantly increase as a function of progressive intrahepatic BDEneu cholangiocarcinoma growth. Serum Postn and Msln levels were determined by duplicate ELISA measurements made on separate serum samples prepared from exsanguinated blood obtained by cardiac puncture from individual rats. These were matched with corresponding liver tumors of different sizes obtained at the same time from the euthanized animals. Bar and linear graphs for (A) Postn and (B) Msln reflect a strong positive correlation between increased liver tumor weight and progressively elevated levels of each serum protein (Postn, $r = 0.998$, $P \leq 0.0001$; Msln, $r = 0.958$, $P \leq 0.01$). Postn was not detected by ELISA in serum samples from normal rats, but normal rat serum gave a very low Msln background value. Each bar represents the mean ± SD. $^{*}P \leq 1 \times 10^{-2}$, $^{**}P \leq 3 \times 10^{-4}$, $^{***}P \leq 1 \times 10^{-6}$; n, number of animals analyzed per group. Inset in B illustrates protein bands of low to higher banding intensities for the ~40-kDa molecular weight form of Msln detected by western blotting of selected whole serum samples diluted 1:10 from rats with BDEneu liver tumors of various sizes from the same animal groups used for the ELISA measurements. LT represents a loaded control sample showing both the 50-kDa and 40-kDa Msln bands detected by western blotting within a whole protein lysate prepared from a 7.5-g BDEneu liver tumor from the same experiment. Protein/well = 20 μg; g is the liver tumor sample wet weight in grams. Abbreviation: LT, liver tumor.

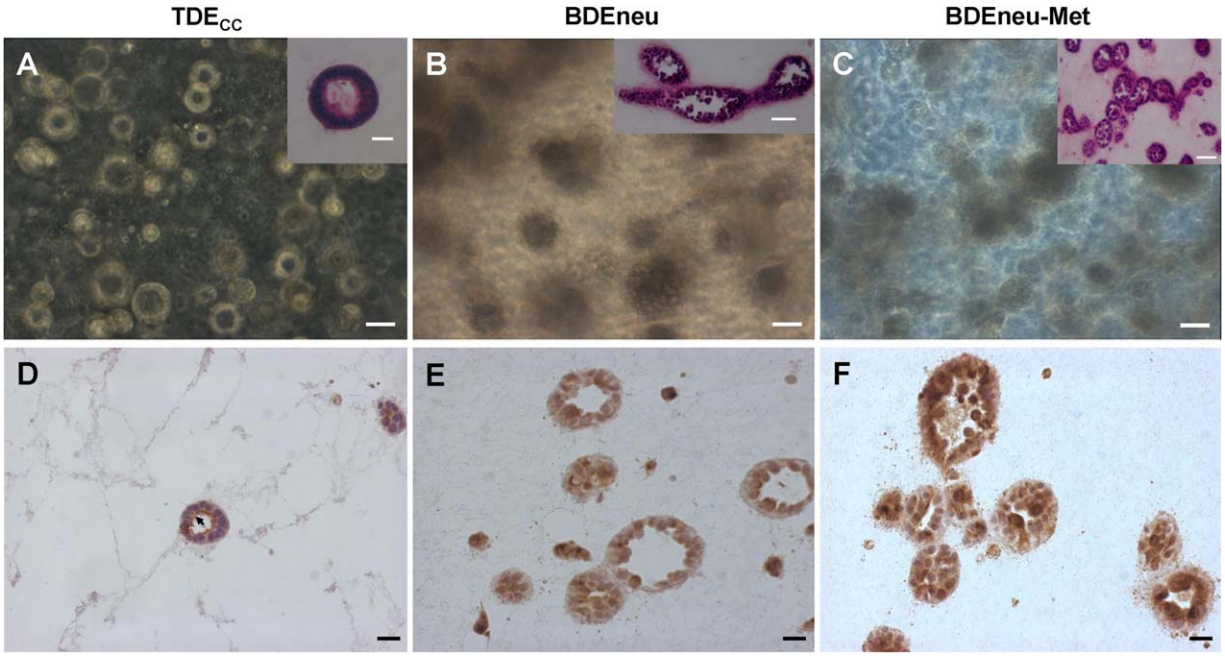

FIG. 5. Msln luminal cell surface versus cytoplasmic immunoreactivity expressed in cholangiocarcinoma cell structures formed in 3-D collagen type I hydrogel cultures distinguish rat cholangiocarcinoma cell types of differing malignant potential and grade. (A) Representative phase contrast photomicrograph demonstrating TDE$_{CC}$ cholangiocarcinoma cells in 3-D culture forming discreet cell spheroids and well-differentiated ductal-like structures with well-circumscribed lumens. (B,C) More highly malignant BDEneu and related BDEneu-Met cholangiocarcinoma cells organize under comparable culture conditions into amorphous-shaped cell clusters or spheroids with irregular borders containing either no or poorly delineated luminal-like spaces. (D) Strongly positive Msln immunoreactivity is localized to the apical/luminal cell surfaces (arrow) of a well-differentiated ductal-like structure formed within the 3-D TDE$_{CC}$ cultures. (E,F) Cholangiocarcinoma cells of the higher malignant cell grade BDEneu and BDEneu-Met structures only exhibited clearly discernable cytoplasmic Msln immunostaining. The cultured TDE$_{CC}$ cell strain, BDEneu, and BDEneu-Met cell lines were each maintained in 3-D gel culture for 12 days (A-C) or 6 days (D-F) under our standard medium conditions and in the continued presence of 10% FBS. The insets in A-C represent corresponding hematoxylin and eosin-stained histologic sections prepared from each gel culture. Magnification bar = 50 μm (A-C, insets B,C) and 20 μm (D-F, inset A). In D-F, nuclei are stained with hematoxylin. Primary Msln antibody dilution = 1: 3,000.

BDEneu liver tumor wet weights. As reflected by the linear relationships (Fig. 3C,D), we determined a strong positive correlation between increasing mean BDEneu liver tumor wet weight and increasing mean relative protein band intensities for Postn ($r = 0.954$; $P = 0.046$) and for the 50-kDa band of Msln ($r = 0.977$; $P = 0.023$). However, the 40-kDa Msln expressed in the liver tumors did not follow this pattern ($r = 0.670$; $P = 0.328$).

That both Postn and Msln may have potential as serum biomarkers for ICC progression prompted us to use ELISA to analyze serum samples from BDEneu cholangiocarcinoma-bearing rats in relation to increasing gross liver tumor wet weight with associated increase in gross peritoneal metastases. The results demonstrated strong positive correlations between increasing serum Postn ($r = 0.998$; $P = 0.0001$) and serum Msln ($r = 0.958$; $P = 0.01$) with increasing mean liver tumor wet weight (Fig. 4A,B). Western blot analysis of serum samples from selected rats bearing BDEneu liver tumors of varying wet weights ranging from low to high predominantly revealed a 40-kDa Msln band expressed at correspondingly lower to higher banding intensities (Fig. 4B inset).

DIFFERENTIAL EXPRESSION OF 50 kDa VERSUS 40 kDa Msln FORMS REFLECT CHOLANGIOCARCINOMA CELL GRADE IN 3-D CULTURE

Using our 3-D rat cholangiocarcinoma culture model, we could show that when cultured alone in

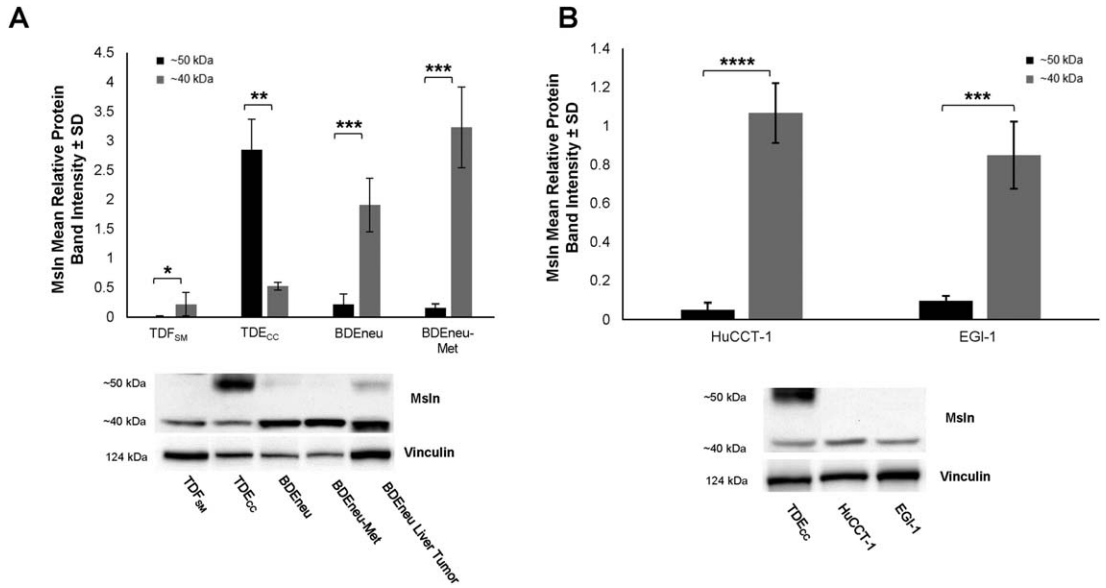

FIG. 6. Differential patterns of 50-kDa versus 40-kDa Msln expression in cultured rat and human neoplastic cholangiocyte/cholangiocarcinoma cell lines/strains of different malignant potential. (A) Quantitative western blot analysis demonstrating the 40-kDa Msln to be the major form detected in total protein lysates from cultured highly malignant BDEneu and BDEneu-Met cell lines. In the less malignantly aggressive TDE_{CC} cell strain, 50-kDa Msln was the predominantly expressed form. Only a low level of expression of the 40-kDa form and no 50-kDa Msln could be detected in comparably cultured TDF_{SM} α-SMA + CAF cells derived from the same cholangiocarcinoma type as the TDE_{CC} cholangiocarcinoma cell strain. (B) Similar to the rat BDEneu and BDEneu-Met cell lines, quantitative western blotting of two separate human cholangiocarcinoma cell lines in monolayer culture showed the 40-kDa Msln as being essentially the only detected form expressed by each cell line. In both A and B, western blots were performed on total protein lysates individually prepared from triplicate monolayer cell cultures in which the cells were grown to confluence on a collagen type I-coated plastic substratum; each bar value represents the mean ± SD. In A, BDEneu liver tumor tissue was also included as a standard. Msln band intensity values were normalized to those of vinculin. $^{*}P \leq 5 \times 10^{-2}$, $^{**}P \leq 2 \times 10^{-3}$, $^{***}P \leq 5 \times 10^{-4}$, $^{****}P \leq 1 \times 10^{-5}$.

dilute collagen type I hydrogel matrix, TDE_{CC} cholangiocarcinoma cells grow in the form of well-circumscribed spheroids, many of which exhibit a ductal-like morphology with distinct lumens (Fig. 5A). In contrast, comparably cultured BDEneu (Fig. 5B) and BDEneu-Met cells (Fig. 5C), are each characterized by the formation of rapidly expanding morphologically disorganized structures of malignant cholangiocytes with irregular borders; this was most expansive in the BDEneu-Met gel cultures.

Strong positive immunoreactivity for Msln could be observed at the apical/luminal surfaces of TDE_{CC} ductal-like structures formed in 3-D gel culture (Fig. 5D), mimicking the pattern of Msln immunostaining exhibited by well-differentiated cholangiocarcinoma ductal structures within TDE_{CC} liver tumor tissue (Fig. 2B). Furthermore, the higher malignant-grade BDEneu and BDEneu-Met cell structures formed in 3-D gel culture predominately showed strong cytoplasmic immunoreactivity for Msln (Fig. 5E,F) and reproduced *in vitro* the pattern of Msln immunostaining exhibited by nests of anaplastic cholangiocarcinoma cells seen in the larger sized BDEneu liver tumors and associated peritoneal metastases.

Using quantitative western blotting, we demonstrated the less malignantly aggressive TDE_{CC} cholangiocarcinoma cells in 3-D gel culture were readily distinguished from the more highly malignant cultured BDEneu and BDEneu-Met cell lines by virtue of their prominent expression of the 50-kDa Msln band relative to that of their significantly lower level of expression of the 40-kDa Msln band (Fig. 6A); in contrast but similar to the BDEneu liver tumor, the BDEneu and BDEneu-Met cell lines each predominantly expressed the 40-kDa Msln band. Moreover, like the BDEneu cell line and tumor, the long-standing human cholangiocarcinoma cell lines analyzed in our study also showed the 40-kDa Msln band to be the predominantly expressed form (Fig. 6B). In comparison,

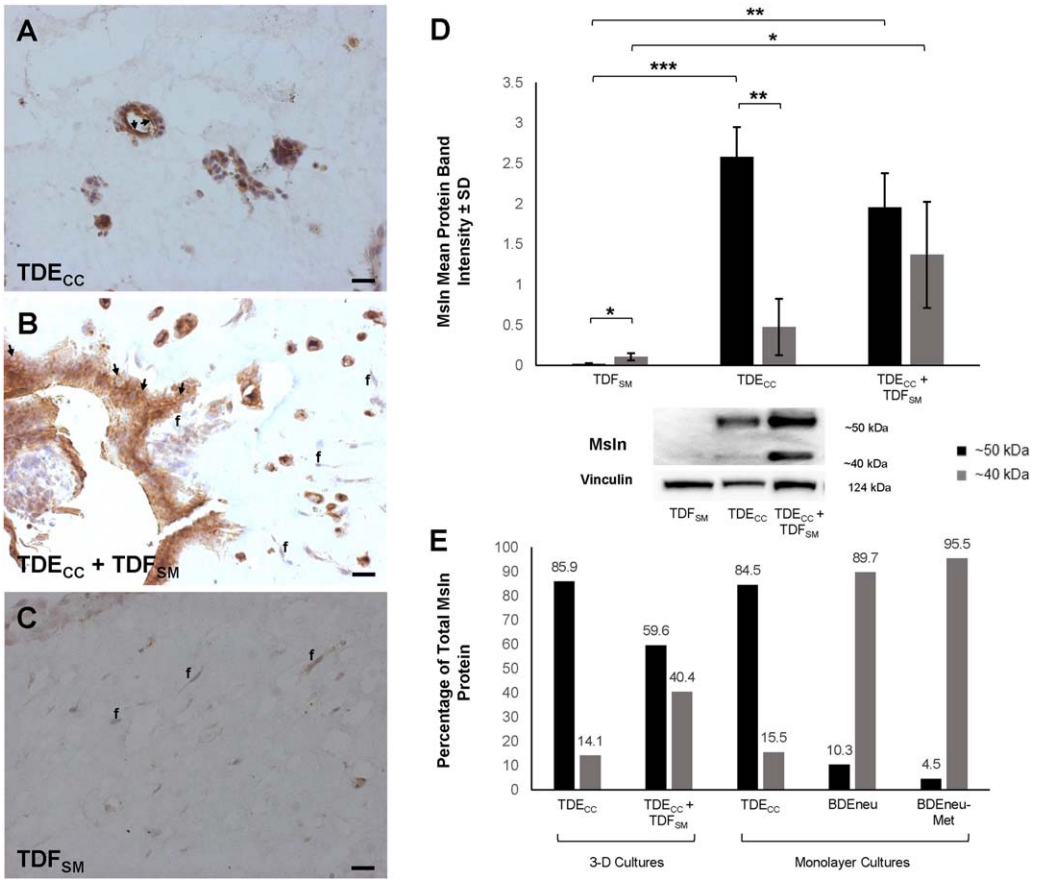

FIG. 7. Coculturing of TDF_{SM} CAFs with TDE_{CC} cholangiocarcinoma cells in 3-D organotypic culture promoting cholangiocarcinoma progression *in vitro* alters cholangiocarcinoma cell Msln immunostaining and 40-kDa versus 50-kDa Msln expression profiles. (A-C) Representative photomicrographs demonstrating differential patterns of Msln immunoreactivity in TDE_{CC} and TDF_{SM} mono-gel cultures compared to the patterns of $TDE_{CC} + TDF_{SM}$ coculture. (A) As demonstrated in Fig. 5D, well-differentiated cholangiocarcinoma ductal-like structures formed within TDE_{CC} the mono-gel culture exhibited a strongly positive apical/luminal cell-surface Msln immunoreactivity (arrows). (B) A less differentiated invasive cholangiocarcinoma cell structure formed when TDF_{SM} cells were cocultured with TDE_{CC} cells in a 3-D collagen gel matrix. The cholangiocarcinoma cells were largely immunoreactive for cytoplasmic Msln, which was markedly more pronounced than that detected in TDF_{SM} cells (f) within the same histologic section. Some cholangiocarcinoma cells also exhibited apparent cell-surface Msln immunostaining (arrows). No Msln immunoreactivity was detected in control sections in which the primary antibody was omitted from the immunostaining reaction mixture. (C) TDF_{SM} cells (f) cultured alone exhibited either no or only weak cytoplasmic immunoreactivity for Msln. Magnification bar for A-C = 20 μm; nuclei stained with hematoxylin. (D) Quantitative western blot analysis demonstrating the 40-kDa Msln form to be significantly increased relative to the 50-kDa form in total protein lysates prepared from the $TDE_{CC} + TDF_{SM}$ gel cocultures when compared with the TDE_{CC} and TDF_{SM} mono-cell gel cultures, respectively. Initial plating density for TDE_{CC} cells = 4×10^5 cells per gel culture and for TDF_{SM} cells = 1.6×10^6 cells/gel. Cultures were maintained for 6 days in standard medium with 10% FBS before total protein extraction for western blotting. Each bar value represents the mean ± SD determined from triplicate cultures. $^{*}P \leq 3 \times 10^{-2}$, $^{**}P \leq 2 \times 10^{-3}$, $^{***}P \leq 3 \times 10^{-4}$. (E) Graphic representation of data depicted in Fig. 7D (3-D culture) and Fig. 6A (monolayer cultures) demonstrating a markedly higher percentage of 40-kDa Msln compared with the 50-kDa form being detected in cell lysates from cultures containing higher grade cholangiocarcinoma cells (BDEneu-Met > BDEneu > $TDE_{CC} + TDF_{SM}$) than in those from cultures of lower grade less aggressive TDE_{CC} cholangiocarcinoma cells alone. Numbers above bars are individual percentage values.

cultured TDF_{SM} CAF cells exhibited only a weak 40-kDa Msln band and no detectable 50-kDa band.

We have recently shown that 3-D coculturing of TDF_{SM} cells with TDE_{CC} cells within dilute collagen type I hydrogels in medium containing 1.0% FBS significantly promotes PCNA-positive cholangiocarcinoma cell spheroidal/ductal-like growth together with a strong desmoplastic-like reaction *in vitro* that mimics that of the *in situ* TDE_{CC} liver tumor.[17] Furthermore, in agreement with our earlier published

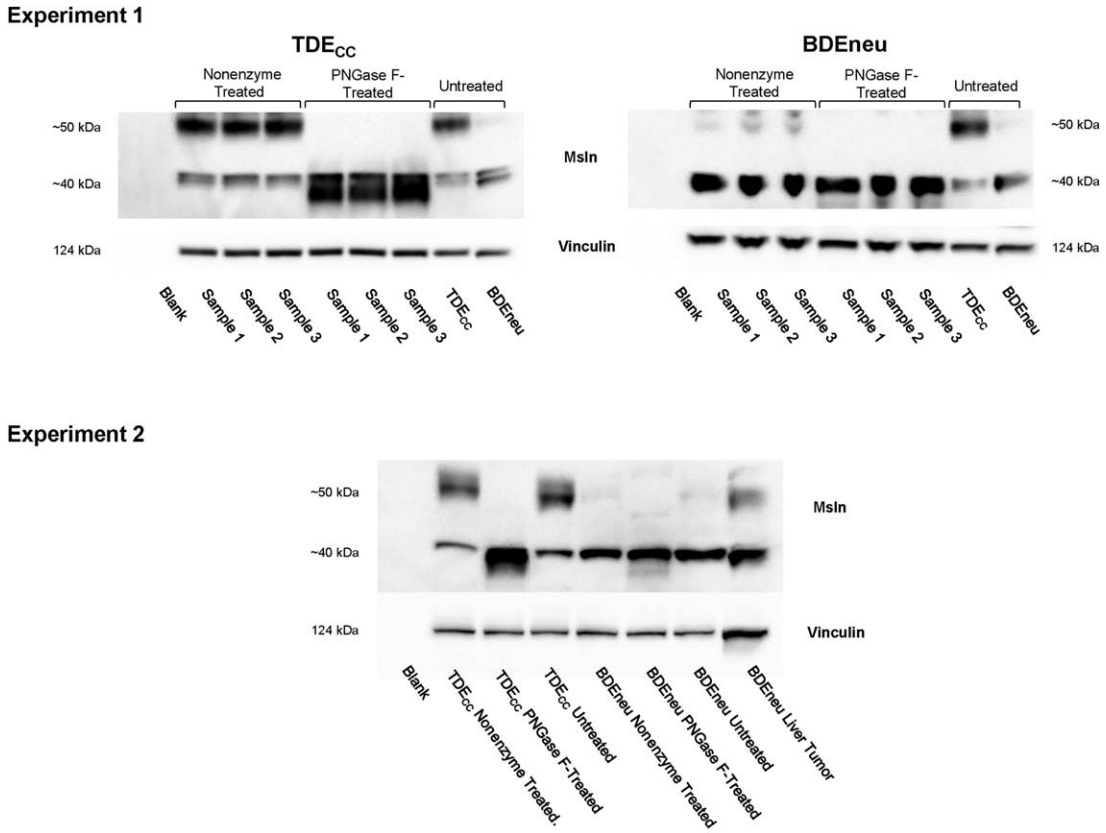

FIG. 8. Deglycosylation treatment converts 50-kDa Msln to its 40-KDa form. Results shown are from two separate experiments. Total protein lysates from TDE_{CC} and BDEneu cells in monolayer culture were treated with PNGaseF. Samples in Experiment 1 refer to those prepared from individual cultures. Nonenzyme-treated samples omitted PNGaseF from the enzyme incubation step. Untreated refers to protein extraction samples prepared directly from the cultured cells without further processing. PNGaseF treatment was without effect on the BDEneu cells because these cells, unlike cultured TDE_{CC} cholangiocarcinoma cells, essentially expressed the 40-kDa Msln form of Msln, with only marginal expression of the 50-kDa form.

findings,[21] increasing the FBS concentration in the medium to 10% enhanced focal areas of cholangiocarcinoma cell anaplasia within cholangiocarcinoma cell + α-SMA + CAF gel cocultures but not within the TDE_{CC} mono-cell gel cultures (Supporting Fig. S3). Confirming our immunostaining results shown in Fig. 5D, strong Msln immunoreactivity was consistently localized to the apical/luminal cell surface of the well-differentiated cholangiocarcinoma ductal-like structures formed within the TDE_{CC} mono-cell gel cultures maintained in 10% FBS-supplemented medium (Fig. 7A). On the other hand, cytoplasmic Msln immunoreactivity was largely discernable in the morphologically disorganized cholangiocarcinoma cell aggregates/clusters commonly observed within histologic sections prepared from the $TDE_{CC} + TDF_{SM}$ gel cocultures (Fig. 7B), although ductal-like structures also seen infrequently in sections from these cocultures showed luminal Msln immunostaining. Weak or no Msln immunostaining was observed within α-SMA + TDF_{SM} cells cultured alone (Fig. 7C) or in coculture with TDE_{CC} cells (Fig. 7B; Supporting Fig. S4). Also of particular significance, the 40-kDa Msln band was seen to be significantly increased relative to that of the 50-kDa Msln band in immunoblots of total protein lysates from $TDE_{CC} + TDF_{SM}$ cocultures, whereas the TDE_{CC} mono-cell gel cultures predominantly expressed 50-kDa Msln (Fig. 7D,E). These latter findings are compatible with the data shown in Fig. 6A for cultured BDEneu and BDEneu-Met cells compared with TDE_{CC} cells; taken together, the data associate loss of luminal Msln immunoreactivity combined with increased expression of 40-kDa Msln to a higher cholangiocarcinoma cell grade and conversely higher 50-kDa Msln expression with strong luminal immunostaining to a lower malignant grade.

CONVERSION OF 50-kDa Msln TO ITS 40-kDa FORM IS DEPENDENT ON ENZYMATIC CLEAVAGE OF GLYCOSYLATION SITES

We postulated that the differences in the migration of both forms of Msln might be related to their degree of glycosylation. To address this possibility, we used western blotting to analyze whole cell lysates from cultured TDE_{CC} and BDEneu cells following treatment with recombinant PNGaseF to remove glycosidic chains. PNGaseF treatment of the cultured TDE_{CC} cells eliminated the 50-kDa band with a concomitant enhancement of the 40-kDa band, whereas this enzymatic treatment had essentially no effect on the cell-specific 40-kDa Msln banding profile characterizing the BDEneu cells (Fig. 8).

Discussion

There is now mounting, albeit still limited, clinical evidence to individually implicate Postn and Msln as each being prognostic for ICC and to suggest their potential as novel molecular targets for ICC therapy. However, while the current findings suggesting Postn and Msln as independent predictors of tumor recurrence and patient survival following ICC resection are compelling, ICC's rarity and typically advanced presentation at the time of diagnosis makes it highly challenging in the clinical setting to experimentally address the biological functions and therapeutic potential of these two distinctive molecular factors in relation to ICC development and progression. In an effort to begin to address the functional and translational significance of Postn and Msln in ICC, we applied quantitative western blotting and ELISA together with immunohistochemistry to evaluate Postn and Msln expression and modulation in preclinical rat cholangiocarcinoma models that closely reproduce key cellular, pathologic, and molecular features of human ICC desmoplasia and progression *in situ* and *in vitro*.

Using a comprehensive immunochemical approach and our "patient-like" orthotopic model of rat cholangiocarcinoma progression, we were able to clearly demonstrate with significant positive correlations increasingly elevated levels of tumor and serum Postn and Msln and enlarging mass-forming cholangiocarcinoma growth in liver with an associated enhancement of gross peritoneal metastases. With respect to human mass-forming ICC, larger tumor size has been reported by some[3,22,23] but not by others [24,25] to independently predict poor recurrence-free survival following curative-intent tumor resection. Our data shown in Fig. 1, which were based on actual wet weight measurements of individual gross liver tumors and associated pooled peritoneal metastases and not on tumor diameter, together with our previously reported time-course data for BDEneu liver and metastatic peritoneal tumor growth *in situ*[16] seem to support the relationship between larger tumor size and increased cholangiocarcinoma progression in this rat cholangiocarcinoma model; however, other markers of increasing malignant progression, including overexpression of activated ErbB2,[16,19] significantly increased mucin 1 expression,[19] higher *in vitro* cell growth rates,[16] and marked increase in the numbers of α-SMA + CAFs accumulated within the desmoplastic tumor stroma,[26] were also previously found by us to associate with the enhanced malignant potential and progression exhibited by highly tumorigenic rat *neu*-transformed cholangiocytes and corresponding BDEneu tumors when compared with low malignant spontaneously transformed rat BDE1 cholangiocytes and corresponding BDEsp tumors.

Increasing numbers of α-SMA + CAFs in the tumor stroma of human and rat BDEneu ICC have been shown to be associated with increased malignant progression.[26,27] Postn immunoreactivity, which has been observed to colocalize with α-SMA immunostaining in human[6] and in rat BDEneu ICCs,[1] was seen by us to be most extensive in the stroma of the more aggressive BDEneu liver cholangiocarcinomas of increasing tumor mass and anaplasia over that observed in the slow growing well-differentiated BDEsp tumors and intermediate growing well-to-moderately differentiated TDE_{CC} tumors. That Postn protein was also determined by both immunohistochemistry and western blotting to be more prominent in the larger sized BDEneu liver tumors than in the smaller BDEneu liver tumors also appears to reflect an increased accumulation of α-SMA + CAFs within the enlarging desmoplastic stroma of the larger sized liver tumors.[1] The likelihood that tumor stromal myofibroblastic cells are the exclusive source of Postn in our models is strongly supported by our previously reported microarray, quantitative reverse-transcription polymerase chain reaction, western blot, and immunofluorescence results demonstrating Postn messenger RNA and protein to be solely expressed in an α-SMA + CAF cell line (BDEsp-TDF) and clonal cell strain (TDF_{SM}) established from an orthotopic rat BDEsp

cholangiocarcinoma but not detected in either tumorigenic BDEneu or BDEsp cell lines nor in BDEsp tumor-derived TDE_{CC} cholangiocarcinoma cells.[17,19] Our results demonstrating a strong positive correlation between increasing levels of both tumor and serum Postn as a function of increasing liver cholangiocarcinoma tumor size, enhanced desmoplastic stroma, and increased gross peritoneal metastases in BDEneu tumor-bearing rats also strongly support stromal Postn overexpression as being predictive of progressive cholangiocarcinoma growth in our rat cholangiocarcinoma model. Our findings are thus compatible with the findings of Utispan et al.[6] and Thuwajit et al.[11] for human ICC. In contrast, rats with biliary cirrhosis induced by bile duct ligation were previously demonstrated by us not to exhibit measurable levels of Postn protein expression by either immunohistochemistry or western blot analysis.[1]

The full-length human Msln gene encodes a 69- to 71-kDa precursor protein that is furin cleaved into a ~40-kDa C-terminal glycosylated fragment (mature Msln; C-ERC) and a 31-kDa N-terminal fragment soluble protein (N-ERC; also termed megakaryocyte potentiating factor). C-ERC is attached to the cell membrane by a glycosylphosphatidylinositol anchor.[28,29] More recently, Zervos et al.[30] detected Msln as a 49-kDa protein in lysates from some mouse tissues and in human embryonic kidney cells (HEK 293 cells) transfected with an Msln-expressing plasmid. This was viewed by these authors as being consistent with the predicted molecular weight of the cleaved mature protein plus glycosylation. Msln shedding from the cell surface of malignant cells has further been shown to be mediated by the sheddase tumor necrosis factor-α-converting enzyme, which is a member of the matrix metalloproteinase/a disintegrin and metalloproteinase family.[31] It has been also shown that a ~40-kDa soluble member of the Msln/megakaryocyte potentiating factor family, first demonstrated in sera from patients with ovarian carcinoma[32] and termed soluble Msln-related protein, is actually shed Msln.[33,34]

In comparison, our western blot analysis revealed both a ~50-kDa and ~40-kDa form of Msln in our analyzed samples of rat cholangiocarcinoma tissues and cell lines/strains. Here, it is relevant that we could show that the Msln antibody used in our study immunoreacted with both the tumor cell 40-kDa and 50-kDa forms of Msln, indicating a commonly shared epitope. Furthermore, similar to others,[9,30] we did not clearly detect evidence of the higher molecular precursor form of Msln (e.g., 69-71 kDa) in our gels, which could possibly indicate that the furin cleavage is rapid.[30] On the other hand, we could show that conversion of the 50-kDa form to the 40-kDa form could be achieved by glycosidase treatment. Moreover, we demonstrated by western blotting that the 40-kDa form was likely the major Msln form being detected in the sera of rats bearing BDEneu tumor. Similar to the western blot findings of others[9] for human ICCs and cholangiocarcinoma cell lines, we observed the 40-kDa Msln to be the predominant form being expressed in the BDEneu tumors and cultured BDEneu cholangiocarcinoma cell line as well as in the two cultured human cholangiocarcinoma cell lines that we analyzed. It is interesting that our immunohistochemical staining largely localized Msln immunoreactivity to the cytoplasm of the BDEneu cells both in culture and *in vivo*, although occasional anaplastic cholangiocarcinoma cells in our study were observed to exhibit apparent cell surface Msln immunoreactivity (i.e., see Fig. 7B; Supporting Fig. S5). In any event, one cannot be certain from our current results that the 40-kDa form measured by western blotting was of a cytoplasmic rather than cell surface membrane origin.

Compatible with the findings of Nomura et al.[7] for human ICC, Msln overexpression in the cholangiocarcinoma cells strongly correlated in our rat model with increasing liver tumor growth and malignant aggressiveness, further suggesting Msln overexpression as being associated with ICC progression. Our results demonstrating increased serum Msln to correlate with increasing tumor size are also in full agreement with the findings of Fukamachi et al.,[35] who reported an interrelationship between the serum Msln level and tumor size in a rat pancreatic cancer model. This latter finding, however, is contrary to that of Sharon et al.,[15] who in an earlier study showed an absence of elevated serum Msln in patients with pancreatic ductal carcinoma, a human cancer known to exhibit high Msln expression. The basis for this discrepancy in results is not clear, although possible explanations might include species and bioassay differences and for the human study, poor shedding and limited tumor bulk, conformational differences in Msln shedding residues, and/or destruction of Msln in the cancer before entry into the blood stream.[15,34] It is also noteworthy that while we were able to demonstrate a strong positive linear correlation between increasing liver tumor size and elevated levels of serum Msln, our analysis of the BDEneu tumor tissue samples revealed only the more highly glycosylated 50-kDa form and not the 40-kDa form measured in the tumors to significantly

correlate with increasing liver tumor mass (Fig. 3D). That tumor Msln expression and serum levels do not strictly correlate has also been reported for human ovarian carcinoma and malignant mesothelioma.[36] One possible explanation that might explain, at least in part, this discrepancy as it relates to our orthotopic BDEneu cholangiocarcinoma model is that the 40-kDa Msln predominant form when released into the expanding CAF-enriched tumor microenvironment is being more rapidly degraded within the larger sized more aggressive BDEneu tumors than in the earlier formed smaller sized tumors; the significantly lower amount of the 50-kDa form expressed in the BDEneu tumors may reflect a more stable form specific to the cholangiocarcinoma cells, thereby selectively discriminating between the cancer cell component and modifying effects of the liver tumor microenvironment. It is also possible that the increased serum Msln levels measured in rats with the larger sized tumors are being augmented by levels being released into blood from peritoneal metastases and/or from cells other than the cholangiocarcinoma cells, such as from peritoneal mesothelial cells in contact with metastatic cholangiocarcinoma cells and/or from Msln-positive intra- or extrahepatic α-SMA + CAFs interacting with invasive/metastatic cancer cells. However, further studies are needed to test these alternative possibilities along with a need to determine if cholangiocarcinoma tumor-derived exosomes containing 40-kDa Msln being released into the blood stream may also be a contributing factor.

Interestingly, we could show that the less aggressive more differentiated cholangiocarcinomas (BDEsp and TDE_{CC} tumors) exhibit strongly positive apical/luminal cell-surface Msln immunostaining, whereas highly malignant, higher grade, metastatic BDEneu tumors primarily showed cytoplasmic Msln immunoreactivity. Similar Msln immunostaining patterns were observed by us for human ICC tissue (Supporting Fig. S5). These rat tumor results are in sharp contrast to the findings of others[37] who reported strong luminal membrane Msln immunostaining in human extrahepatic bile duct cancers to more significantly correlate with liver and peritoneal metastases and with a more unfavorable patient survival outcome, while patients whose tumors expressed cytoplasmic Msln without luminal membrane staining had a more favorable prognosis. Even more compelling is our finding that the 50-kDa form of Msln was expressed at significantly higher levels compared to the 40-kDa form in the less aggressive BDEsp and TDE_{CC} cholangiocarcinomas *in situ* and polarized TDE_{CC} structures formed in 3-D culture that express apical/luminal Msln cell-surface immunoreactivity; the highly tumorigenic and more malignantly aggressive orthotopic BDEneu liver tumors and associated peritoneal metastases and the corresponding BDEneu and BDEneu-Met cell lines, characterized by cytoplasmic Msln immunostaining, loss of cell polarity, and increased anaplasia, significantly overexpressed 40-kDa Msln compared to the 50-kDa form. Taken together, these results indicate that a predominant overexpression of the heavily glycosylated 50-kDa form of Msln compared to the 40-kDa form, coupled with strong immunoreactivity at the apical luminal cell surface of cholangiocarcinoma cells, is predictive of a more differentiated, less aggressive, malignant phenotype in both our orthotopic and 3-D rat cholangiocarcinoma models. Conversely, significantly elevated expression of 40-kDa Msln compared to the 50-kDa form, together with increased cytoplasmic Msln immunostaining, is predictive of increased malignant progression. In this context, it also appears relevant that stably transfecting the mouse Panc02 pancreatic cancer line to overexpress 49-kDa murine Msln at the cell surface has been reported to not increase cell proliferation or anchorage-independent growth *in vitro* and most surprisingly to inhibit tumor formation *in vivo* in immunocompetent mice.[30]

Expanding on our liver tumor results, we were able to demonstrate that 3-D coculturing α-SMA + CAFs (TDF_{SM} cells) with cholangiocarcinoma cells (TDE_{CC} cells) under culture conditions that enhanced cholangiocarcinoma cell growth and progression *in vitro* led to a notable decrease in apical/luminal Msln immunostaining with an increase in cytoplasmic Msln immunoreactivity. This occurred together with a measurable decrease in the expression of 50-kDa Msln and a corresponding increase in the 40-kDa form that correlated with an increase in cholangiocarcinoma cell anaplasia and loss of ductal-like cell polarity *in vitro* when compared with TDE_{CC} cells cultured without TDF_{SM} cells. This novel finding is significant not only because it reproduces in cell culture our *in situ* tumor findings but also because it demonstrates the modulating effect of α-SMA + CAFs on changing the Msln expression profile to reflect that of a more aggressive cholangiocarcinoma phenotype. It remains to be determined if the modulation of Msln is an epiphenomenon associated with cholangiocarcinoma progression or whether CAFs interacting with cholangiocarcinoma cells provoke particular mechanisms contributing to the increase in the 40-kDA Msln form over the 50-kDa form that determine the changing pattern of expression

of Msln. One intriguing avenue to explore in attempting to provide mechanistic insight for this change is the investigation of regulators of cell polarity and disruption of protein signaling mechanisms that regulate apical-basal polarity[38] on Msln isoform expression patterns in relation to increasing cholangiocarcinoma cell anaplasia.

Our extensive characterization of the TDF_{SM} and TDE_{CC} cell strains used in this study strongly supports a resident liver mesenchymal cell origin of the TDF_{SM} cells, which are not neoplastically transformed, and a pure cholangiocarcinoma cell origin of the tumorigenic TDE_{CC} cells without evidence of epithelial mesenchymal transition.[17] Moreover, we also demonstrated by transcriptomic analysis and by immunophenotyping that the α-SMA + TDF_{SM} CAFs prominently overexpress gene products (e.g., gremlin, cell surface Thy-1, fibulin 2, cofilin 1) that have been shown to be overexpressed in activated portal fibroblasts relative to activated hepatic stellate cells.[17] Our current data further support the cholangiocarcinoma cells and not the activated CAF myofibroblasts as being the major source of Msln expressed in both the orthotopic cholangiocarcinomas and in the 3-D cocultures. The conditional ablation of Msln-activated portal fibroblasts expressing mature 40-kDa Msln or therapeutic administration of anti-Msln-blocking antibodies has been reported to attenuate BDL-induced liver fibrosis in mice,[39] suggesting that Msln may be a potential target for antifibrotic therapy. However, our findings appear to argue against CAF Msln playing a major role in regulating the desmoplastic response in ICC or its potential as an antifibrotic target for depleting α-SMA + CAFs from ICC stroma.

While there have been many studies carried out on the functions of Msln and Postn, their role in cancer progression, including that of ICC, remains unclear and needs to be elucidated.[8,34,40] Based on the data described herein, we propose that our unique rat cholangiocarcinoma models are ideal preclinical platforms for investigating Postn and Msln biology, regulation and functional relationships in the context of α-SMA + CAF and cancer cell interactions promoting ICC progression, and the potential of Postn and Msln as molecular targets for ICC therapy.

REFERENCES

1) Sirica AE, Dumur CI, Campbell DJ, Almenara JA, Ogunwobi OO, DeWitt JL. Intrahepatic cholangiocarcinoma progression: prognostic factors and basic mechanisms. Clin Gastroenterol Heptol 2009;7(Suppl.):S68-S78.
2) Sirica AE, Gores GJ. Desmoplastic stroma and cholangiocarcinoma: clinical implications and therapeutic targeting. Hepatology 2014;59:2397-2402.
3) Mavros MN, Economopoulos KP, Alexiou VG, Pawlik TM. Treatment and prognosis for patients with intrahepatic cholangiocarcinoma: systematic review and meta-analysis. JAMA Surg 2014;149:565-574.
4) Rizvi S, Borad MJ, Patel T, Gores GJ. Cholangiocarcinoma: molecular pathways and therapeutic opportunities. Semin Liver Dis 2014;34:456-464.
5) Wirth TC, Vogel A. Surveillance in cholangiocellular carcinoma. Best Pract Res Clin Gastroenterol 2016;30:987-999.
6) Utispan K, Thuwajit P, Abiko Y, Charngkaew K, Paupairoj A, Chau-in S, et al. Gene expression profiling of cholangiocarcinoma-derived fibroblast reveals alterations related to tumor progression and indicates periostin as a poor prognostic marker. Mol Cancer 2010;9:13.
7) Nomura R, Fujii H, Abe M, Sugo H, Ishizaki Y, Kawasaki S, et al. Mesothelin expression is a prognostic factor in cholangiocellular carcinoma. Int Surg 2013;98:164-169.
8) Sirica AE, Almenara JA, Li C. Periostin in intrahepatic cholangiocarcinoma: pathobiological insights and clinical implications. Exp Mol Pathol 2014;97:515-524.
9) Yu L, Feng M, Kim H, Phung Y, Kleiner DE, Gores GJ, et al. Mesothelin as a potential therapeutic target in human cholangiocarcinoma. J Cancer 2010;1:141-149.
10) Fujimoto K, Kawaguchi T, Nakashima O, Ono J, Ohta S, Kawaguchi A, et al. Periostin, a matrix protein, has potential as a novel serodiagnostic marker for cholangiocarcinoma. Oncol Rep 2011;25:1211-1216.
11) Thuwajit C, Thuwajit P, Jamjantra P, Pairojkul C, Wongkham S, Bhudhisawasdi V, et al. Clustering of patients with intrahepatic cholangiocarcinoma based on serum periostin may be predictive of prognosis. Oncol Lett 2017;14:623-634.
12) Ordóñez NG. Application of mesothelin immunostaining in tumor diagnosis. Am J Surg Pathol 2003;27:1418-1428.
13) Ruys AT, Groot Koerkamp B, Wiggers JK, Klümpen HJ, ten Kate FJ, van Gulik TM. Prognostic biomarkers in patients with resected cholangiocarcinoma: a systematic review and meta-analysis. Ann Surg Oncol 2014;21:487-500.
14) Higashi M, Yamada N, Yokoyama S, Kitamoto S, Tabata K, Koriyama C, et al. Pathobiological implications of MUC16/CA125 expression in intrahepatic cholangiocarcinoma-mass forming type. Pathobiology 2012;79:101-106.
15) Sharon E, Zhang J, Hollevoet K, Steinberg SM, Pastan I, Onda M, et al. Serum mesothelin and megakaryocyte potentiating factor in pancreatic and biliary cancers. Clin Chem Lab Med 2012; 50:721-725.
16) Sirica AE, Zhang Z, Lai GH, Asano T, Shen XN, Ward DJ, et al. A novel "patient-like" model of cholangiocarcinoma progression based on bile duct inoculation of tumorigenic rat cholangiocyte cell lines. Hepatology 2008;47:1178-1190.
17) **Manzanares MÁ**, **Usui A**, **Campbell DJ**, Dumur CI, Maldonado GT, Fausther M, et al. Transforming growth factor α and β are essential for modeling cholangiocarcinoma desmoplasia and progression in a three-dimensional organotypic culture model. Am J Pathol 2017;187:1068-1092.
18) Lai GH, Zhang Z, Shen XN, Ward DJ, DeWitt JL, Holt SE, et al. erbB-2/neu transformed cholangiocytes recapitulate key

cellular and molecular features of human bile duct cancer. Gastroenterology 2005;129:2047-2057.
19) Dumur CI, Campbell DJ, DeWitt JL, Oyesanya RA, Sirica, AE. Differential gene expression profiling of cultured neu-transformed versus spontaneously-transformed rat cholangiocytes and of corresponding cholangiocarcinomas. Exp Mol Pathol 2010;89:227-235.
20) Yang L, Faris R, Hixson DC. Long-term culture and characteristics of normal rat liver bile duct epithelial cells. Gastroenterology 1993;104:840-852.
21) Campbell DJ, Dumur CI, Lamour NF, DeWitt JL, Sirica AE. Novel organotypic culture model of cholangiocarcinoma progression. Hepatol Res, 2012;42:1119-1130.
22) Endo I, Gonen M, Yopp AC, Dalal KM, Zhou Q, Klimstra D, et al. Intrahepatic cholangiocarcinoma: rising frequency, improved survival, and determinants of outcome after resection. Ann Surg 2008;248:84-96.
23) Lin ZY, Liang ZX, Zhuang PL, Chen JW, Cao Y, Yan LX, et al. Intrahepatic cholangiocarcinoma prognostic determination using pre-operative serum C-reactive protein levels. BMC Cancer 2016;16:792.
24) DeOliveira ML, Cunningham SC, Cameron JL, Kamangar F, Winter JM, Lillemoe KD, et al. Cholangiocarcinoma: thirty-one-year experience with 564 patients at a single institution. Ann Surg 2007;245:755-762.
25) Choi SB, Kim KS, Choi JY, Park SW, Choi JS, Lee WJ, et al. The prognosis and survival outcome of intrahepatic cholangiocarcinoma following surgical resection: association of lymph node metastasis and lymph node dissection with survival. Ann Surg Oncol 2009;16:3048-3056.
26) Sirica AE, Campbell DJ, Dumur CI. Cancer-associated fibroblasts in intrahepatic cholangiocarcinoma. Curr Opin Gastroenterol 2011;27:276-284.
27) Okabe H, Beppu T, Hayashi H, Horino K, Masuda T, Komori H, et al. Hepatic stellate cells may relate to progression of intrahepatic cholangiocarcinima. Ann Surg Oncol 2009;16:2555-2564.
28) Hassan R, Remaley AT, Sampson ML, Zhang J, Cox DD, Pingpank J, et al. Detection and quantitation of serum mesothelin, a tumor marker for patients with mesothelioma and ovarian cancer. Clin Cancer Res 2006;12:447-453.
29) Kelly RJ, Sharon E, Pastan I, Hassan R. Mesothelin-targeted agents in clinical trials and in preclinical development. Mol Cancer Ther 2012;11:517-525.
30) Zervos E, Agle S, Freistaedter AG, Jones GJ, Roper RL. Murine mesothelin: characterization, expression, and inhibition of tumor growth in a murine model of pancreatic cancer. J Exp Clin Cancer Res 2016;35:39.
31) Zhang Y, Chertov O, Zhang J, Hassan R, Pastan I. Cytotoxic activity of immunotoxin SS1P is modulated by TACE-dependent mesothelin shedding. Cancer Res 2011;71:5915-5922.
32) Scholler N, Fu N, Yang Y, Ye Z, Goodman GE, Hellström KE. Soluble member(s) of the mesothelin/megakaryocyte potentiating factor family are detectable in sera from patients with ovarian carcinoma. Proc Natl Acad Sci U S A 1999;96:11531-11536.
33) Ho M, Onda M, Wang QC, Hassan R, Pastan I, Lively MO. Mesothelin is shed from tumor cells. Cancer Epidemiol Biomarkers Prev 2006;15:1751.
34) Pastan I, Hassan R. Discovery of mesothelin and exploiting it as a target for immunotherapy. Cancer Res 2014;74:2907-2912.
35) Fukamachi K, Iigo M, Hagiwara Y, Shibata K, Futakuchi M, Alexander DB, et al. Rat N-ERC/mesothelin as a marker for in vivo screening of drugs against pancreas cancer. PLoS One 2014; 9:e111481.
36) Scholler N. Mesothelin. In: Schwab M, ed. Encyclopedia of Cancer, Volume 3. 3rd ed. Berlin, Heidelberg, Germany: Springer; 2011;2241-2245.
37) Kawamata F, Kamachi H, Einama T, Homma S, Tahara M, Miyazaki M, et al. Intracellular localization of mesothelin predicts patient prognosis of extrahepatic bile duct cancer. Int J Oncol 2012;41:2109-2118.
38) Halaoui R, McCaffrey l. Rewiring cell polarity in cancer. Oncogene 2015;34:939-950.
39) Koyama Y, Wang P, Liang S, Iwaisako K, Liu X, Xu J, et al. Mesothelin/mucin 16 signaling in activated portal fibroblasts regulates cholestatic liver fibrosis. J Clin Invest 2017;127:1254-1270.
40) Liu AY, Zheng H, Ouyang G. Periostin, a multifunctional matricellular protein in inflammatory and tumor microenvironments. Matrix Biol 2014;37:150-156.

Author names in bold designate shared co-first authorship.

Supporting Information

Additional Supporting Information may be found at onlinelibrary.wiley.com/doi/10.1002/hep4.1131/full.